



Giant Intracranial Cavernous Malformations: A Review on Magnetic Resonance Imaging Characteristics

Mustafa Kemal Demir¹ Deniz Kilic² Emre Zorlu² Turker Kilic²

¹ Clinic of Radiology, Bahcesehir University Goztepe Medical Park Hospital, Istanbul, Turkey

² Department of Neurosurgery, Bahcesehir University School of Medicine, Göztepe Medical Park Hospital, Istanbul, Turkey

Address for correspondence Mustafa Kemal Demir, MD, 11. kısım, Yasemin Apartment, D-Block. Daire 35 Ataköy 34158, Istanbul, Turkey (e-mail: demir.m.k@gmail.com).

Indian J Radiol Imaging 2024;34:511–521.

Abstract

Background Intracranial cavernous malformations (CMs), commonly known as cavernomas or cavernous angiomas, are low-flow, well-circumscribed vascular lesions composed of sinusoidal spaces lined by a single layer of endothelium and separated by a collagenous matrix without elastin, smooth muscle, or other vascular wall elements. A diameter greater than 3 cm for a CM is unlikely. These lesions may have atypical appearances on magnetic resonance imaging (MRI). MRI with advanced techniques such as a susceptibility-weighted image or T2-gradient echo, a diffusion-weighted image and corresponding apparent diffusion coefficient map, and diffusion tensor tractography have revolutionized the diagnostic approach to these lesions.

Materials and Method The present study reviews the etiopathogenesis, clinical manifestations, MRI strategy, and MRI appearances of the CMs, with a few examples of the giant CMs from our archive.

Results Intracranial giant CMs may have unexpected locations, sizes, numbers, and varied imaging appearances due to repeated hemorrhages, unusual enhancement patterns, intense perifocal edema, and unusual associations, making the differential diagnosis difficult.

Conclusion Familiarity with the MRI appearances of the giant intracranial CMs and the differential diagnosis improves diagnostic accuracy and patient management.

Keywords

- ▶ cavernous malformation
- ▶ cavernoma
- ▶ cavernous angioma
- ▶ giant
- ▶ magnetic resonance imaging

Introduction

According to McCormick's classification, intracranial vascular malformations include cavernous malformations (CMs), arteriovenous malformations, developmental venous anomalies (DVAs), and capillary telangiectasias. Both arteriovenous malformations and CMs have increased angiogenic potential.¹ The CMs are distinguished from the others by the presence of

well-defined masses composed of numerous sinusoidlike capillary vascular channels of variable size close to each other and lined by a single layer of endothelium with no elastic membrane, smooth muscle cells, intervening parenchyma, or different expression of various angiogenesis-related gene products in cerebral vascular malformations.² The blood flow through these vessels is slow. Hyaline degeneration, thrombosis, cholesterol clefts, calcifications, and hemorrhages

article published online
February 28, 2024

DOI <https://doi.org/10.1055/s-0044-1779587>.
ISSN 0971-3026.

© 2024. Indian Radiological Association. All rights reserved.
This is an open access article published by Thieme under the terms of the Creative Commons Attribution-NonDerivative-NonCommercial-License, permitting copying and reproduction so long as the original work is given appropriate credit. Contents may not be used for commercial purposes, or adapted, remixed, transformed or built upon. (<https://creativecommons.org/licenses/by-nc-nd/4.0/>)
Thieme Medical and Scientific Publishers Pvt. Ltd., A-12, 2nd Floor, Sector 2, Noida-201301 UP, India

may also be associated with these masses. Since CMs are vascular tumors, they are also referred to as cavernous hemangiomas, cavernomas, or cavernous angiomas. They can be divided into intra- and extra-axial types. Their histological findings are almost identical but distinct in magnetic resonance imaging (MRI) studies.

In this article, our aim is to review the etiopathogenesis, clinical features, MRI strategies, and the MRI appearances of the disease, a brief differential diagnosis, and treatment options focusing on the giant CMs larger than 3 cm.

Etiopathogenesis

CMs most commonly occur sporadically in about 80% of the population with no gender predisposition or run in families randomly. Although both the sporadic and hereditary forms are histopathologically similar, some triggering or precipitating factors leading to the formation of the vascular lesion may exist. The association with DVA (previously known as venous angioma) plays an important role in the pathogenesis of sporadic CMs. A study with 7-T MRI showed an association between all sporadic CMs and a small venous anomaly.³ Additionally, contrast-enhanced MRI studies in patients with evidence of DVA demonstrate an increased prevalence of CM that is strongly correlated with age.⁴ It has been hypothesized that venous hypertension associated with DVA leads to red cells passing into the extracellular space. On the other hand, increased intraluminal pressure within the DVA causes reduced tissue perfusion resulting in hypoxia. Thus, the process of local angiogenesis may initiate and cause the growth of CMs.⁵⁻⁷ Recognition of the coexistence of CMs and the DVA is crucial since associated CMs may have a greater tendency to bleed and be symptomatic than isolated ones.⁸ In addition to the association with DVA, factors related to the de novo formation of CMs include previous radiation therapy, a brain biopsy, viral infection, and hormonal influences, especially in pregnancy.^{5,9-11} The majority of patients with familial form do not have an associated DVA and typically present with multiple lesions. The familial forms of CMs have an autosomal dominant inheritance pattern with variable expression and incomplete penetrance and are caused by mutations in CCM1 (KRIT1) on chromosome 7q, CCM2 (MGC4607) on chromosome 7p, or CCM3 (PDCD10) on chromosome 3q.^{12,13} However, some of the familial cases cannot be explained by these three known genes, suggesting the existence of additional loci. The products of these genes are critical to angiogenesis and the loss of their function leads to the development of abnormal vascular structures characterized by thin-walled and dilated blood vessels with gaps between the endothelial cells.¹⁴

Clinical Presentations

A large percentage of patients with CM have no apparent symptoms and are generally discovered as an incidental lesion when a brain MRI is done for an unrelated purpose. When symptoms are present, these depend on the CM size,

location, and complications arising from the lesion. The most common clinical manifestations of CM are headache, epileptic seizure, neurological problems such as a hemorrhagic stroke, limb weakness, vision problems, dysarthria, dizziness, difficulty concentrating, and memory problems. Since they are dynamic lesions, a rapid expansion may also be associated with neurological symptoms. Extra-axial CMs such as cavernous sinus hemangiomas have different clinical pictures, natural history, and imaging findings with tumor-like behavior including the enclosure of neurovascular structures.^{15,16}

Magnetic Resonance Imaging Strategy

MRI is the preferred imaging modality for the detection and characterization of CMs with the highest sensitivity and specificity.¹⁷ Magnetic field strength and pulse sequences are particularly important. Studies indicate that 3-T field strength increases sensitivity to detect CMs when compared to 1.5-T field strength.⁸ On ultrahigh field strength (≥ 7.0 T), sensitivity increases even further.¹⁸ Conventional MRI sequences are essential in the differential diagnosis since CMs are generally well characterized due to their distinct appearance on T1-weighted images (T1WIs) and T2-weighted images (T2WIs). T2-gradient echo sequences or susceptibility-weighted imaging (SWI) should be specifically included in the imaging protocol since they are sensitive sequences for the detection of CMs. However, these sequences are also very sensitive to cerebral microbleeds in various disorders, such as amyloid angiopathy, chronic hypertensive encephalopathy, radiation therapy, hemorrhagic metastasis, and traumatic injury. Thus, parenchymal CMs may be indistinguishable from cerebral microbleeds on MRI.¹⁹ It should also be emphasized that type IV parenchymal CMs are only visible on SWIs as hypointense dots, similar to cerebral microbleeds, and have been reported as a distinct imaging appearance in patients with familial cerebral CMs.^{20,21} Diffusion-weighted imaging (DWI) may have added value in the imaging evaluation of the CMs. Uncomplicated CMs show very low signal intensity on DWI and corresponding apparent diffusion coefficient (ADC) map due to old hemorrhage showing a blackout effect. This imaging modality may also help diagnose recent hemorrhage in patients with hemorrhagic complications showing restricted diffusion inside. Although there is typically no enhancement, CMs may show minimal to prominent enhancement after contrast administration. Contrast-enhanced MRI may also improve the detection of the DVA and simplify the differential diagnosis. Advanced MRI modalities such as diffusion tensor imaging, functional MRI, and perfusion MRI may provide advantages for specific purposes and are usually useful in intraoperative imaging.^{17,22} Perfusion imaging could be used as a diagnostic biomarker in CMs with symptomatic hemorrhages, whereas permeability and perfusion derivations could be used as a prognosis biomarker to predict future bleeding or growth.²³ Digital subtraction catheter angiography is not recommended for evaluation of CMs but may be considered to rule out an arteriovenous malformation.

Table 1 MRI features-based types of cerebral CMs and histopathologic correlation¹⁹

| Type | MRI signals | | | Histopathology |
|------|--|--|--|---|
| | T1-weighted signal intensity | T2-weighted signal intensity | Signal intensity on SWI or T2 gradient echo sequence | |
| I | Hyperintense | Heterogeneous signals with a hypointense rim | Hypointense | Subacute hemorrhage surrounded by hemosiderin stain macrophages and gliotic brain |
| II | Heterogenous with classic “popcorn” appearance | Heterogenous with classic “popcorn” appearance | Hypointense | Loculated areas of hemorrhage and thrombosis of varying age surrounded by hemosiderin-stained brain and gliosis |
| III | Hypointense and isointense | Hypointense and isointense | Hypointense | Chronic resolved hemorrhage with hemosiderin staining within and around the lesion |
| IV | Poorly seen tiny, often multiple, punctate foci with low signals | Poorly seen tiny, often multiple, punctate foci with low signals | Hypointense | Multiple areas of hemosiderin deposition without a central core |

Abbreviations: CM cavernous malformation; MRI magnetic resonance imaging; SWI susceptibility-weighted imaging.

Magnetic Resonance Imaging Appearances

CMs are usually found in the brain parenchyma but may also be seen in the intracranial extra-axial locations. Intracranial uncomplicated parenchymal lesions demonstrate well-defined, characteristic “berry” or “popcorn” like lesions on MRI with a central core of mixed signal intensity surrounded by a rim of signal hypointensity, which demonstrate prominent blooming on susceptibility-weighted sequences. CMs have already been classified into four types depending on hemorrhages in the lesion: type I, subacute hemorrhage surrounded by hemosiderin-stained macrophages, and gliotic brain with hyperintense signals on T1WI and heterogeneous signals with a hypointense rim on T2WI; type II, loculated areas of hemorrhage and thrombosis of varying age surrounded by hemosiderin-stained brain and gliosis with classic “popcorn” appearance and heterogeneous signals on both T1WI and T2WI; type III, hypointense and isointense on T1WI and T2WI due to chronic resolved hemorrhage with hemosiderin staining within and around the lesion; and type IV, often multiple areas of hemosiderin deposition without a central core showing tiny,

punctate, foci hypointensity on both T1WI and T2WI, but best seen on SWI or gradient echo sequences (► **Table 1**).¹⁹

Approximately 75% of the CMs are in the supratentorial region. The cerebral cortex, subcortical white matter, and deep white matter are the most common locations for the disease (► **Table 2**).^{24,25} The rare location, large size, intense enhancement pattern, cystic degeneration, and severe perifocal edema may create unusual appearances on MRI with diagnostic challenges.

A diameter greater than 3 cm for a CM is unlikely and there is no agreed definition of a “giant” CM, but mostly supposed to be greater than 4 or 6 cm.^{26,27} They are extremely rare, and their MRI findings can be different from those of typical CM, making them a diagnostic challenge. They may present as a multicystic lesion with a “bubbles of blood” appearance or with a “salt and pepper” appearance.²⁶ However, these findings are not constant in all the giant CMs. The MRI appearance is variable, but the presence of hemosiderin, blood degradation products, and calcification may be helpful in the diagnosis (► **Fig. 1**). The term “giant” is not intended to discourage or contraindicate surgery.

Table 2 The locations of the cavernous malformations²⁴

| Location | | | | |
|-------------------|-----|--------------------------|-----|------------|
| Supratentorial | % | Posterior fossa | % | Spinal (%) |
| Frontal | 29 | Pons | 8 | 5 |
| Temporal | 18 | Cerebellum | 5 | |
| Parietal | 10 | Medulla oblongata | 3 | |
| Occipital | 6 | Fourth ventricle | 2.3 | |
| Basal ganglia | 4 | Mesencephalon | 1.3 | |
| Sylvian fissure | 3 | Internal acoustic meatus | 0.3 | |
| Lateral ventricle | 2 | | | |
| Corpus callosum | 1.3 | | | |
| Insular | 1.3 | | | |
| Third ventricle | 0.7 | | | |
| Parasellar | 0.7 | | | |

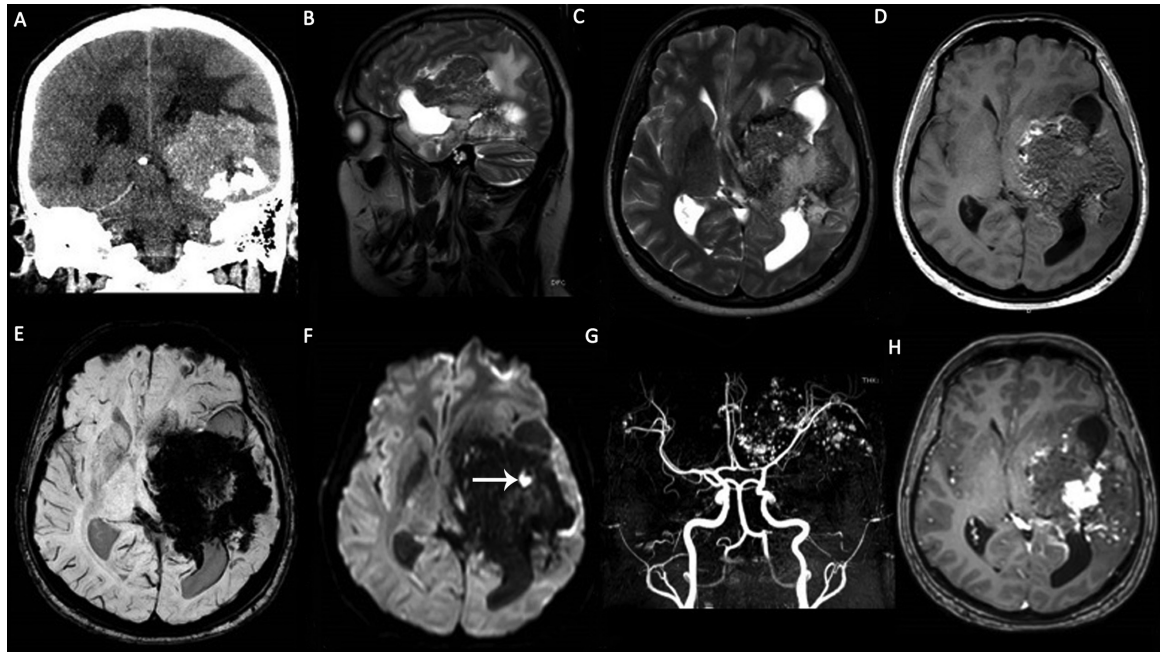


Fig. 1 A left cerebral hemisphere giant cavernous malformation (CM) in a 33-year-old male patient with seizure and headache. (A) Coronal computed tomography (CT) scan demonstrates a large heterogeneous calcified mass in the left cerebral hemisphere. (B) Sagittal T2-weighted image (T2WI), (C) axial T2WI and (D) axial T1WI show that the mass demonstrates heterogeneous signals with “salt and pepper” appearance on nonenhanced T1WI. (E) Susceptibility-weighted imaging (SWI) demonstrates intense “blooming artifacts” due to calcifications and chronic hemorrhage. (F) The mass is mainly hypointense on diffusion-weighted imaging (DWI) and includes a focal-restricted diffusion due to a recent hemorrhage (arrow). (G) Axial view of the maximum intensity projection (MIP) of the time-of-flight magnetic resonance (MR) angiography shows the cavernoma vessels in the left cerebral hemisphere. (H) Contrast-enhanced T1WI demonstrates heterogeneous enhancement.

A cortical CM with a large diameter, prominent perifocal edema, and enhancement on contrast-enhanced T1WI is another unusual appearance of the disease. It may simulate a tumor and may have an important role in the occurrence of epilepsy, a most valid indication for surgical resection (→ Fig. 2). Evaluating the relationship between CM and nearby white matter tracts with diffusion tensor tractography is useful in making a decision on surgical strategies (→ Fig. 3).²⁸

The epileptogenicity of mesiotemporal archicortical involvement is significantly higher than that of extramesiotemporal localization and can also occur as a giant CM with an unusual MRI appearance (→ Fig. 4).²² The T1 hyperintense perilesional signal intensity sign is a very useful imaging finding in distinguishing CMs from other hemorrhagic masses, such as primary or secondary brain neoplasia and primary intracerebral hematoma, although not specifically. This sign is present in approximately two-thirds of cerebral CMs with overt hemorrhage and perilesional edema.^{29–31} The exact origin of the bleeding may go unnoticed due to overt hemorrhages, which can completely mask MRI signs of underlying pathology, particularly CMs. However, the presence of several episodes of recurrent bleeding, a hemosiderin ring, and encapsulation provides evidence for a CM, while the presence of expansile hemorrhage, single-aged blood products, and mass effect argues against the diagnosis of CM. Therefore, we recommend a follow-up MRI within 3 months and at least 6 weeks after the blood has completely

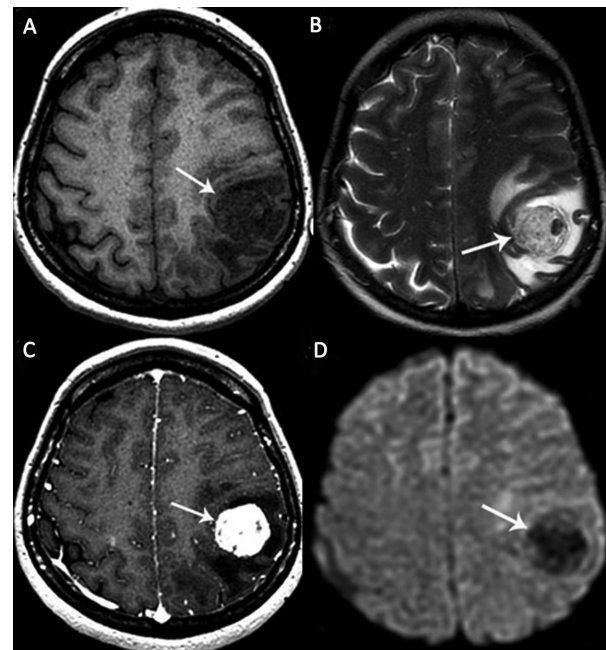


Fig. 2 A left parietal lobe cavernous malformation (CM) in a 41-year-old female patient with a headache. (A) Axial T1-weighted magnetic resonance (MR) image shows a hypointense heterogeneous cortical mass. (B) Axial T2-weighted MR image shows a “berrylike” mass with heterogeneous hypointense and hyperintense signals (arrow). There is a prominent perifocal edema. (C) The mass shows intense heterogeneous enhancement on contrast-enhanced T1-weighted MR image (arrow). (D) The mass is hypointense on diffusion-weighted imaging (DWI) without any restricted diffusion (arrow).

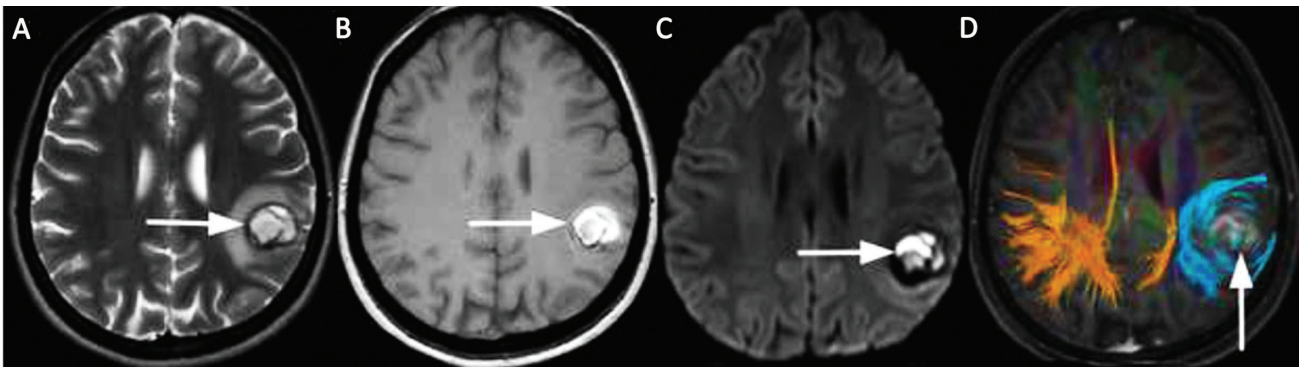


Fig. 3 A left parietal lobe cavernous malformation (CM) in a 25-year-old female patient with seizure. (A) There is a heterogeneous hyperintense lesion with peripheral hypointense rim (*arrow*) and perilesional edema on axial T2-weighted magnetic resonance (MR) image. (B) The lesion shows hyperintense signals on axial T1-weighted MR image, with T1 perilesional hyperintense sign (*arrow*). (C) There is restricted diffusion as hyperintense signals on diffusion-weighted imaging (DWI; *arrow*) and hypointense signals on the corresponding apparent diffusion coefficient (ADC) map (not shown) due to subacute hemorrhage. (D) Diffusion tensor imaging tractography for preoperative planning demonstrates the benign displacement of subcortical white matter fiber tracts (*arrow*).

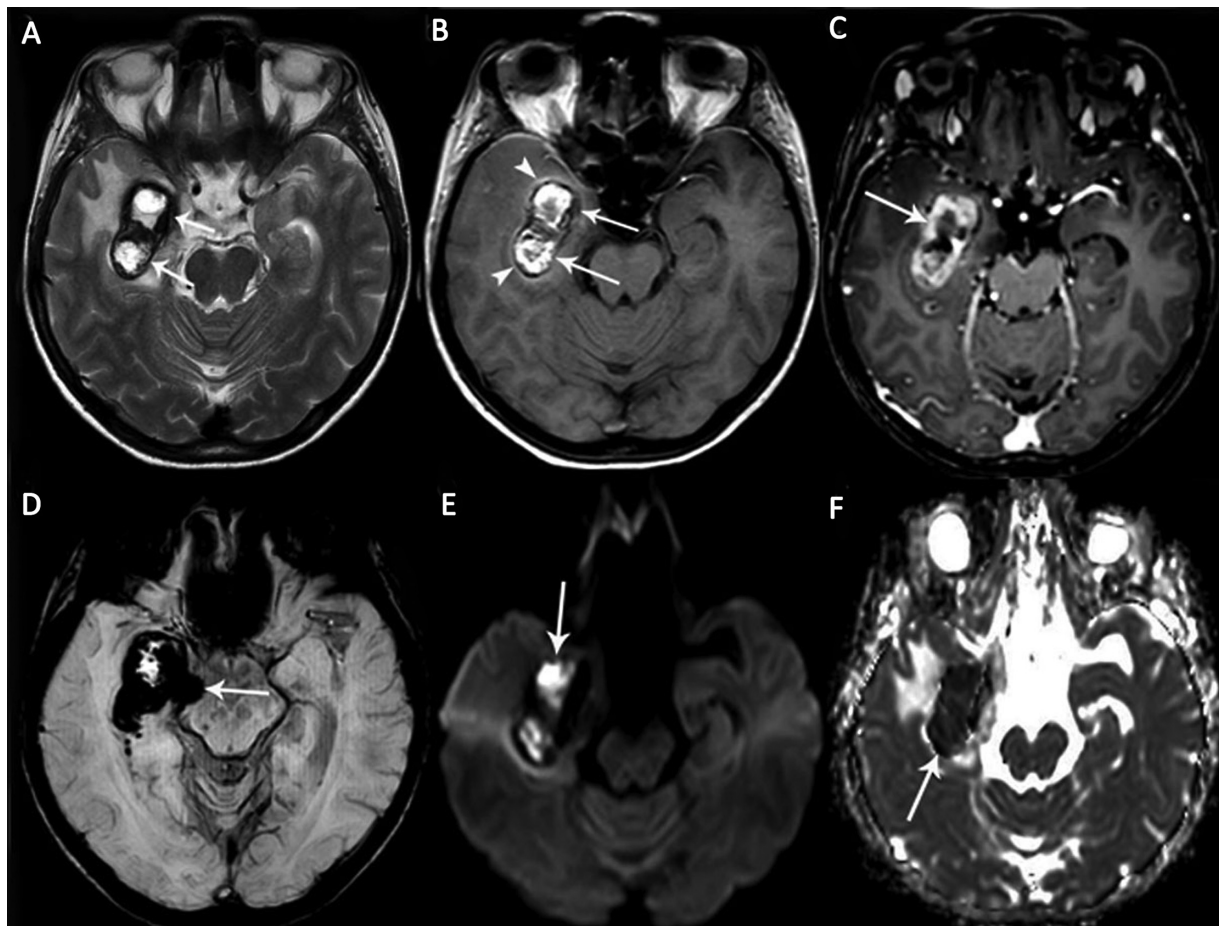


Fig. 4 A right mesial temporal lobe cavernous malformation (CM) in a 42-year-old female patient with epilepsy. Axial (A) T2-weighted and (B) T1-weighted magnetic resonance (MR) images show hyperintense heterogeneous signals surrounded by a hypointense hemosiderin rim (*arrows*). There is the perilesional hyperintense sign on the axial T1-weighted MR image (*arrowheads*). (C) The mass shows intense peripheral enhancement on contrast-enhanced T1-weighted MR image (*arrow*). (D) There is a prominent inhomogeneous hypointense blooming artifact on susceptibility-weighted imaging (SWI) due to hemorrhage in the CM (*arrow*). The mass shows restricted diffusion as (E) hyperintense signals on diffusion-weighted imaging (DWI) and (F) hypointense signals on the corresponding apparent diffusion coefficient (ADC) map due to recent hemorrhage (*arrows*).

lysed. Repeat MRI studies may then be necessary if patients continue to exhibit symptoms or show notable development.

CMs can exhibit multiplicity and simulate metastases. In several patients, they can be of different ages and have

different imaging findings in the MRI. Two adjacent CMs may rarely communicate with each other via a DVA (– Fig. 5). Subcortical CMs can rarely cause epilepsy. A deep location of a giant CM in the basal ganglia, thalamus, hypothalamus,

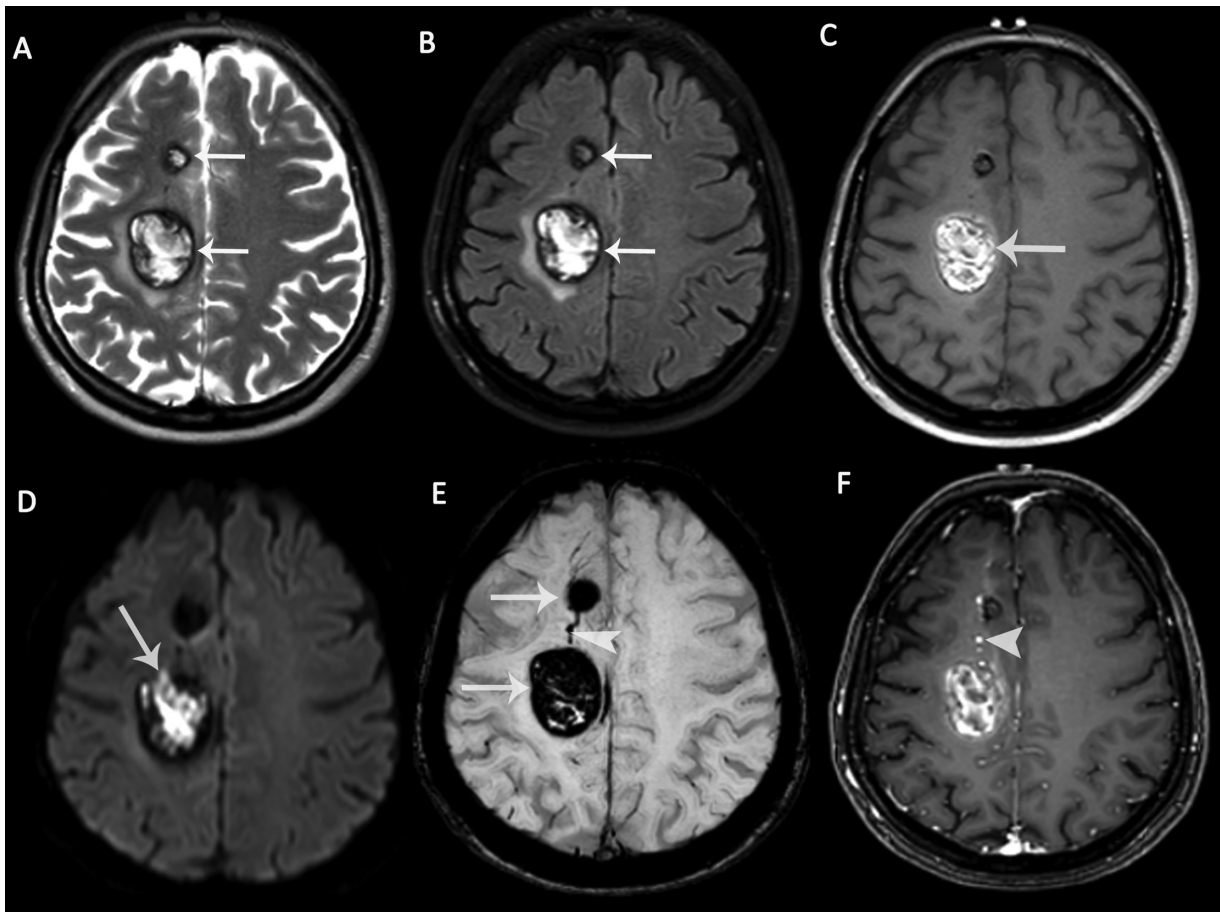


Fig. 5 Magnetic resonance imaging (MRI) of a 40-year-old female patient with multiple cavernous malformations (CMs). Axial (A) T2-weighted image (T2WI) and (B) fluid attenuated inversion recovery (FLAIR) image demonstrate two CMs adjacent to each other, showing typical peripheral hemosiderin rim (arrows) with heterogeneous internal signals. There is perilesional edema around the larger one. (C) The larger one is heterogeneously hyperintense on nonenhanced T1-weighted image (T1WI) due to intralésional subacute hemorrhage (arrow). (D) Diffusion-weighted imaging (DWI) shows hyperintense signals within the larger CM due to diffusion restriction (arrow). (E) The CMs are markedly hypointense on susceptibility-weighted imaging (SWI) due to “blooming artifacts” (arrows). There is a developmental venous anomaly (DVA) between the two cavernomas (arrowhead). (F) Enhancement is not seen in CMs on the contrast-enhanced T1WI, while DVA shows enhancement (arrowhead).

insula, corpus callosum, or paraventricular white matter is infrequent and may pose a preoperative diagnostic challenge (→ Fig. 6).

Posterior fossa CMs represent 7.8 to 35.8% of all cases and the brainstem is the most common site.^{11,32} There is no

difference in the imaging appearance when comparing supratentorial to infratentorial giant CMs. Infratentorial CMs are classified into cerebellar and brainstem CMs, being extremely important for therapeutic planning. CMs can sometimes be associated with subarachnoid hemorrhage

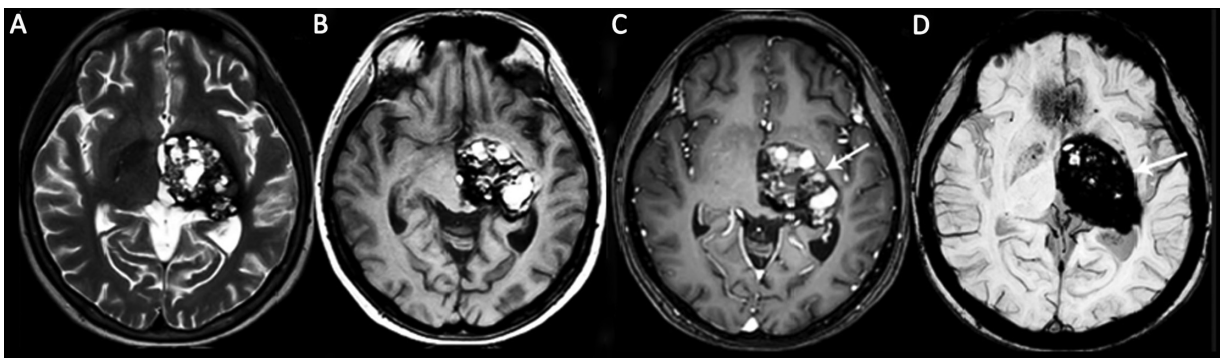


Fig. 6 A left thalamus giant cavernous malformation (CM) in a 25-year-old female patient with a headache and progressive right-sided weakness. (A) Axial T2-weighted (T2W) and (B) T1W magnetic resonance (MR) images show a complex-appearing mass with heterogeneous signals and cystic areas. (C) Contrast-enhanced T1-weighted image (TIWI) shows heterogeneous internal enhancement (arrow). (D) Susceptibility-weighted imaging (SWI) shows an intense inhomogeneous blooming artifact (arrow).

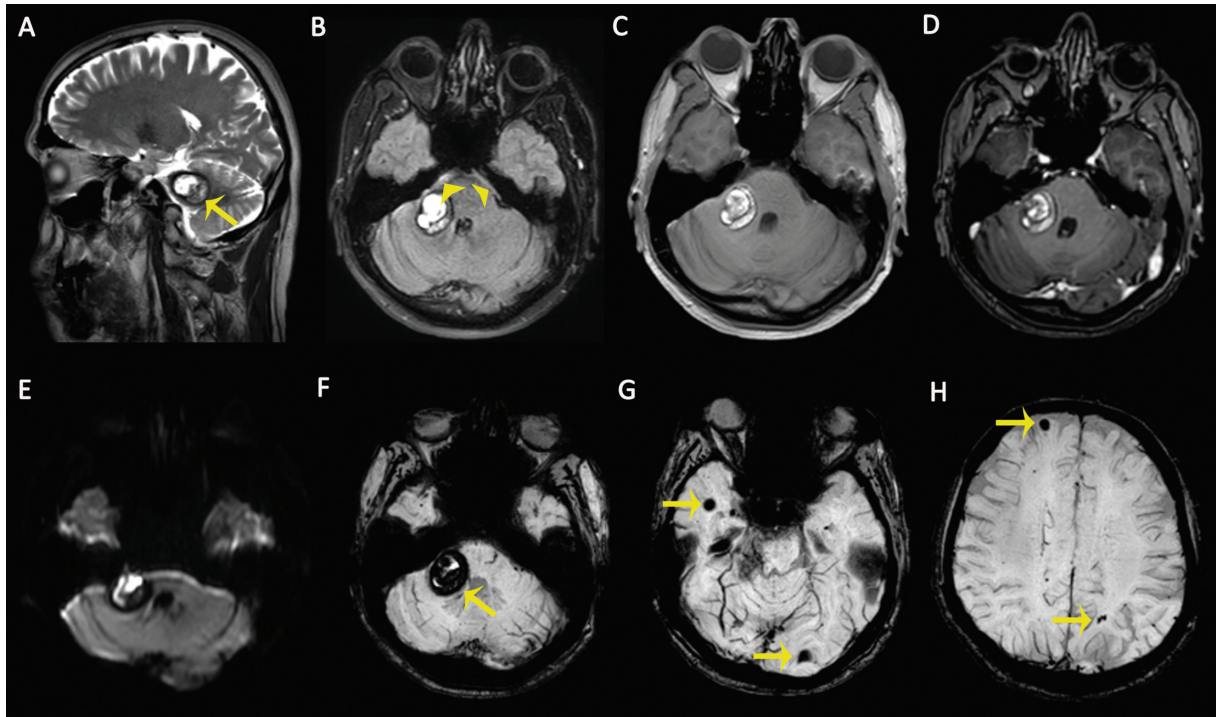


Fig. 7 Magnetic resonance (MR) images of a 42-year-old male patient with an acute severe headache. (A) Sagittal T2-weighted image (T2WI) demonstrates a cavernous malformation (CM) in the cerebellopontine angle with peripheral hypointense hemosiderin ring (arrow). (B) Axial fluid-attenuated inversion recovery (FLAIR) sequence demonstrates a CM and perimesencephalic subarachnoid hemorrhage (arrowheads). (C) The lesion is heterogeneously hyperintense on nonenhanced T1-weighted image (T1WI) due to intralesional recent hemorrhage. (D) No enhancement was observed on axial contrast-enhanced T1WI. (E) Recent hemorrhages within the CM cause diffusion restriction on diffusion-weighted imaging (DWI) as hyperintense signals. (F–H) Susceptibility-weighted images (SWIs) show multiple intracranial CMS with “blooming artifacts” (arrows).

that is angiographically negative (–Fig. 7).³³ Brainstem CMs, like the other sites, are associated with high risks of bleeding and rebleeding, resulting in a rapid enlargement and neurological morbidity (–Fig. 8). Once a cavernoma has bled, the annual rebleeding rate increases.³⁴

Extra-axial CMs may rarely be found in intraventricular, subarachnoid, subdural, and epidural areas. Epidural CMs are thought to arise from the venous plexus of the dura and represent 5% of all CMs.^{35,36} Most of the extra-axial CMs have been found in the middle cranial fossa with or without cavernous sinus extension. Other locations may include the dural sinuses, falx cerebri, tentorium, dura in the cranial

nerve foramen, cerebellopontine angle, and convexity dura.^{37,38}

It should be emphasized that cerebral CMs and cavernous sinus hemangiomas exhibit some histological differences. The presence of a capsule or pseudocapsule and the absence of previous hemorrhage are the main characteristics of cavernous sinus hemangiomas. They contain vascular channels that lack histological evidence of thrombosis and calcification.³⁹ Thus, extra-axial CMs are usually seen as uniform hypointense to cortical gray matter on T1WI, typically brightly hyperintense on T2WI, and show intense homogeneous enhancement on contrast-enhanced T1WI with

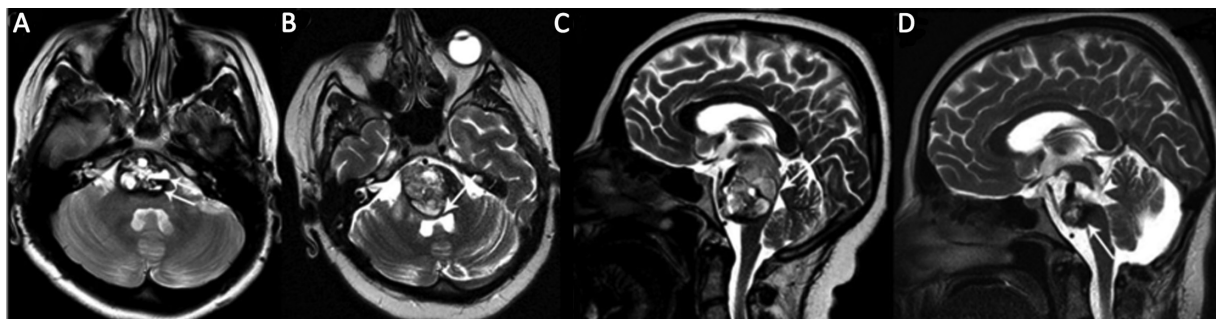


Fig. 8 A pontine cavernous malformation (CM) in a 27-year-old female patient with headache and ataxia. (A) Axial T2-weighted magnetic resonance (MR) image shows a pontine CM with cystic components, showing hematocrit levels (arrow). (B) Axial and (C) sagittal T2-weighted MR images show a prominent progression of the lesion in the 6-month follow-up period after Gamma Knife surgery treatment, causing fourth ventricle compression (arrows). (D) Sagittal T2-weighted postoperative MR image shows partially resected CM (arrow) and postoperative porencephaly (arrowhead).

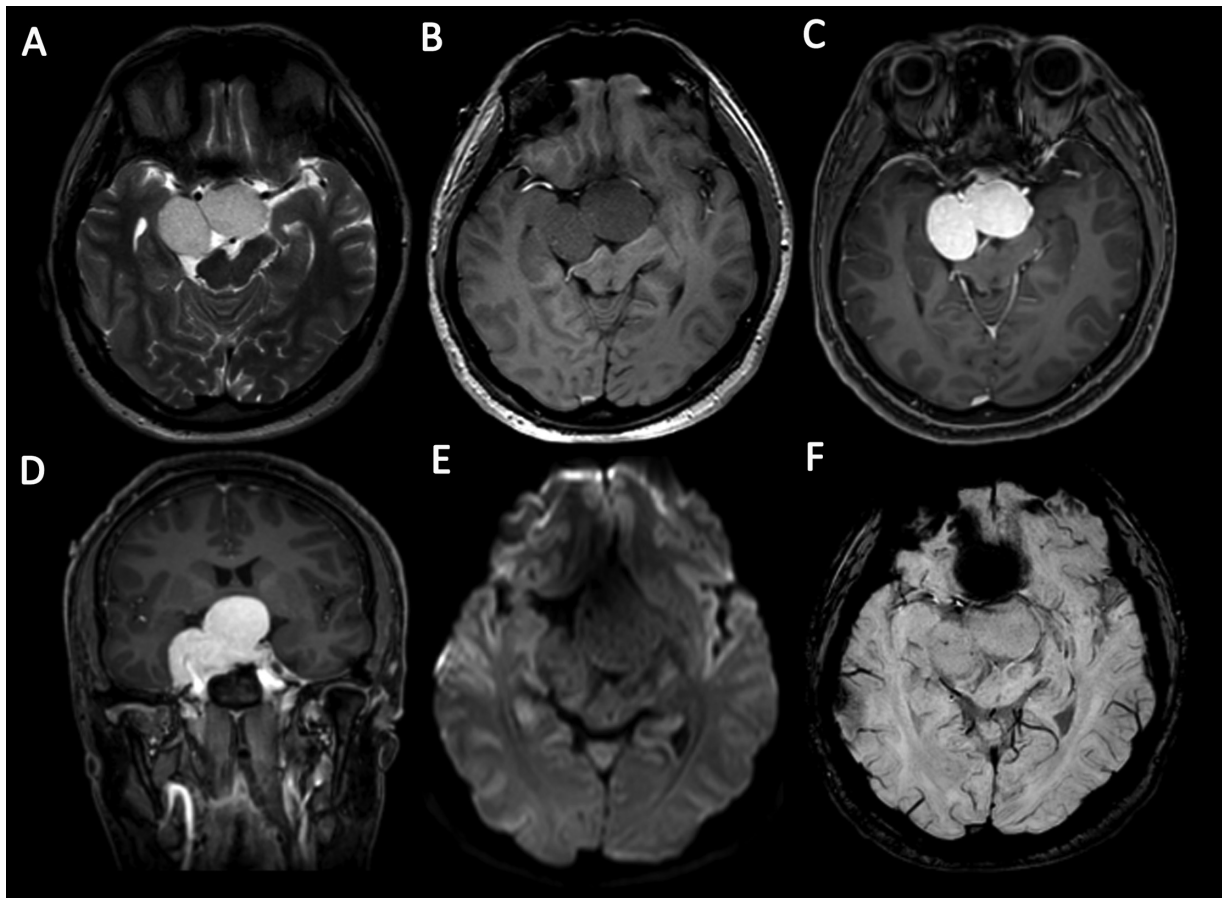


Fig. 9 A right cavernous sinus cavernous hemangioma extending to the intrasellar and suprasellar areas in a 37-year-old male patient with a history of progressive headache and blurring of vision. (A) Axial T2-weighted image (T2WI) demonstrates a large lobulated shape mass with a homogeneous hyperintense signal compressing the optic chiasm. The mass (B) is hypointense on axial T1-weighted image (T1WI) and (C) shows homogeneous intense enhancement on contrast-enhanced axial T1WI and (D) contrast-enhanced coronal T1WI. (E) No diffusion abnormality is detected on diffusion-weighted imaging (DWI). (F) There is no “blooming artifact” on susceptibility-weighted imaging (SWI).

well-defined boundaries but without a “dural tail” sign (→Fig. 9). The main distinctions between cerebral and dural CMs are outlined in →Table 3. The differential diagnosis of the dural CMs include meningiomas and schwannomas. Intra- and extra-axial CMs can be seen together in the same patient and the presence of associated congenital anomaly or syndrome needs to be investigated (→Figs. 10 and 11).^{3,40,41} On the other hand, CMs may also be observed with other intracranial disorders such as cortical dysplasia, glioma, meningioma, or other vascular anomalies, either as a coexistence or as a collision tumor.^{42–44}

Treatment

Conservative management with yearly serial imaging and observation is the treatment of choice for small and incidentally discovered CMs. Indications for surgery may include multiple hemorrhages, neurological deficits, and progressive seizures unless the location carries an unacceptably high surgical risk. Low-dose Gamma Knife radiosurgery is a valid option for small CMs that provides adequate seizure control and improved quality of life carrying a low risk of treatment complications without

Table 3 Basic distinctions between cerebral and dural cavernous malformations (CMs)

| | Inheritance | Location | Clinical presentation | No. of lesions | Hemosiderin ring | Recurrence |
|--------------|--------------------|---|--|-------------------------------|------------------|------------|
| Cerebral CMs | Autosomal dominant | Most frequently supratentorial | Seizures, focal hemorrhagic neurological impairments | Multiple in familial patients | Present | Common |
| Dural CMs | Sporadic | Most frequently found in middle cranial fossa and cavernous sinus | Headache, cranial nerve palsies, or mass effect-related neurological abnormalities | Single | Absent | Rare |

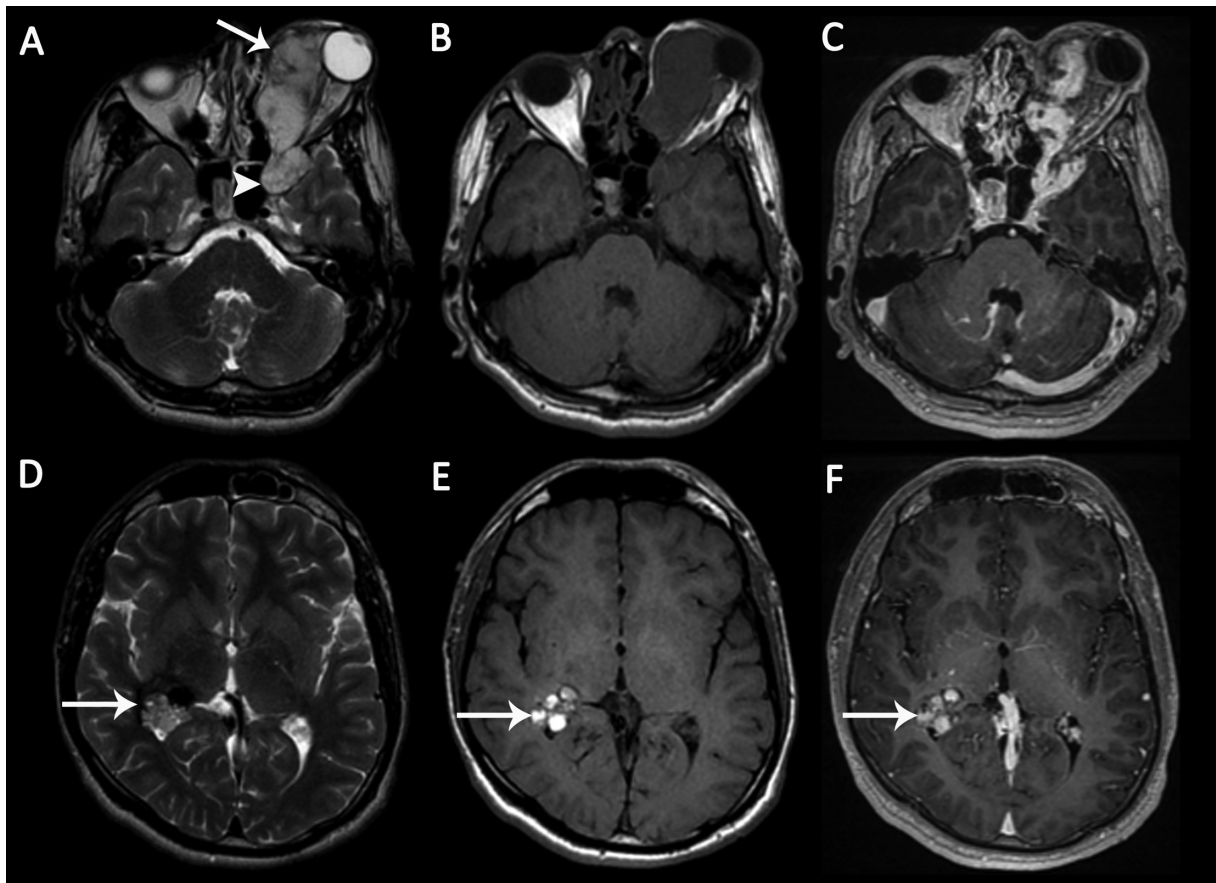


Fig. 10 Large cavernous malformation in a 20-year-old male patient with painless proptosis of the left eye. (A) Axial T2-weighted image (T2WI) demonstrates a left orbital lobulated heterogeneous hyperintense lesion (arrow), extending to the anterior part of the left cavernous sinus (arrowhead). (B) The mass is hypointense on axial T1-weighted image (T1WI). (C) The mass shows early nonhomogeneous intense enhancement. Axial (D) T2WI and (E) axial T1WI demonstrate an incidental intraventricular cavernoma with cystic components in the right trigon (arrows). There are hemorrhagic signals within the lesion. (F) There is no enhancement on axial contrast-enhanced T1WI (arrow).

any adverse radiation effects. The risk of hemorrhage and the neurological deficits associated with hemorrhage in patients with brainstem CMs are greater than those in other patients with CMs located elsewhere. The annual rebleeding rate for brainstem and nonbrainstem cerebral CMs was 11 and 6.8%, respectively, in a research on morbidity following symptomatic cerebral CM hemorrhage. In brainstem CM, the overall morbidity was 31.3%, while in the nonbrainstem subgroup, it was 21%. Of the total participants in the research, 15.6% still needed daily help due to a moderate or severe impairment. Among the brainstem group, the moderate to severe morbidity rate was 18.8%, whereas in nonbrainstem CCM, it was 12.3%.⁴⁵

Patients with giant CMs may be initially managed with antiepileptic medications. However, surgical resection is advised for progressive seizure and neurological disability. When a DVA is present alongside CM, this should be left intact. Complete surgical removal of the CM is required, because of the risk of hemorrhage or seizure recurrence.⁴⁶⁻⁴⁸ CMs in deep locations require a technically cautious surgery

because of the presence of critical neuronal pathways. CMs that are deep seated and surgically inaccessible seem to benefit from stereotactic or Gamma Knife radiosurgery owing to a reduction of annual hemorrhage rate in the first 2 years.⁴⁹⁻⁵¹

Conclusion

Intracranial giant CMs constitute a heterogeneous group of vascular malformations with varied MRI characteristics but still with identical histopathologic features. Current neuroimaging techniques, especially MRI with advanced techniques such as SWI or T2-gradient echo, DWI and corresponding ADC map, and diffusion tensor tractography, have revolutionized the diagnostic approach to these lesions. Familiarity with these unusual MRI appearances of intracranial CMs and the differential diagnosis improves diagnostic accuracy and patient management.

Funding
None.

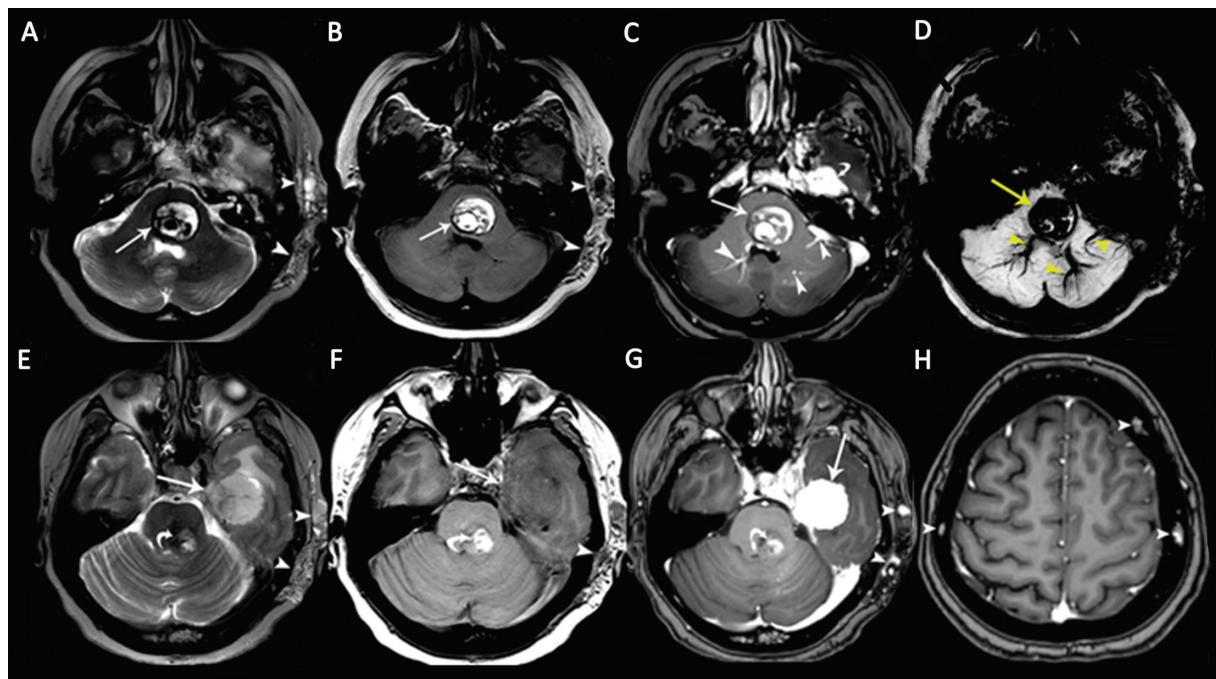


Fig. 11 A 48-year-old woman patient with multiple cavernous malformations (CMs) associated with a cavernous sinus hemangioma. Axial (A) T2-weighted image (T2WI) and (B) T1-weighted image (T1WI) show a pontine CM with heterogeneous signals and peripheral hemosiderin deposits (arrows) associated with soft-tissue hemangioma in the left temporal subcutaneous area (arrowheads). (C) Contrast-enhanced axial T1WI shows nonenhancing CM (arrow), enhancing developmental venous anomalies (DVAs; arrowheads) in the brainstem, and an enhancing dural cavernous hemangioma in the left middle cranial fossa (curved arrow). (D) Pontine CM and DVAs show “blooming artifacts” on susceptibility-weighted imaging (SWI). (E) Axial T2WI shows a large dural cavernous hemangioma in the left middle cranial fossa with heterogeneous hyperintense signals (arrow). There is also a brainstem CM (curved arrow) and a soft-tissue hemangioma in the left temporal subcutaneous area (arrowheads). (F) The dural cavernous hemangioma in the left middle cranial fossa is hypointense on the axial T1WI. The soft-tissue hemangioma in the left temporal subcutaneous tissue is hypointense on the image (arrowhead). (G) The dural cavernous hemangioma in the left middle cranial fossa shows intense homogeneous enhancement on contrast-enhanced T1WI (arrow). The brainstem CM shows no enhancement (curved arrow). Soft-tissue hemangioma in the left temporal subcutaneous tissue shows a few dotlike enhancing areas, representing dilated veins. (H) Axial contrast-enhanced T1WI shows multiple calvarial CMs (arrowheads).

Conflict of Interest

None declared.

References

- Konya D, Yildirim O, Kurtkaya O, et al. Testing the angiogenic potential of cerebrovascular malformations by use of a rat cornea model: usefulness and novel assessment of changes over time. *Neurosurgery* 2005;56(06):1339–1345, discussion 1345–1346
- Bicer A, Guclu B, Ozkan A, et al. Expressions of angiogenesis associated matrix metalloproteinases and extracellular matrix proteins in cerebral vascular malformations. *J Clin Neurosci* 2010; 17(02):232–236
- Dammann P, Wrede KH, Maderwald S, et al. The venous angioarchitecture of sporadic cerebral cavernous malformations: a susceptibility weighted imaging study at 7 T MRI. *J Neurol Neurosurg Psychiatry* 2013;84(02):194–200
- Brinjikji W, El-Masri AE, Wald JT, Flemming KD, Lanzino G. Prevalence of cerebral cavernous malformations associated with developmental venous anomalies increases with age. *Childs Nerv Syst* 2017;33(09):1539–1543
- Ciricillo SF, Dillon WP, Fink ME, Edwards MS. Progression of multiple cryptic vascular malformations associated with anomalous venous drainage. Case report. *J Neurosurg* 1994;81(03):477–481
- Maeder P, Gudinchet F, Meuli R, de Tribolet N. Development of a cavernous malformation of the brain. *AJNR Am J Neuroradiol* 1998;19(06):1141–1143
- Ogilvy CS, Moayeri N, Golden JA. Appearance of a cavernous hemangioma in the cerebral cortex after a biopsy of a deeper lesion. *Neurosurgery* 1993;33(02):307–309, discussion 309
- Abdulrauf SI, Kaynar MY, Awad IA. A comparison of the clinical profile of cavernous malformations with and without associated venous malformations. *Neurosurgery* 1999;44(01):41–46, discussion 46–47
- Baumgartner JE, Ater JL, Ha CS, et al. Pathologically proven cavernous angiomas of the brain following radiation therapy for pediatric brain tumors. *Pediatr Neurosurg* 2003;39(04): 201–207
- Flocks JS, Weis TP, Kleinman DC, Kirsten WH. Dose-response studies to polyoma virus in rats. *J Natl Cancer Inst* 1965;35(02): 259–284
- Porter RW, Detwiler PW, Spetzler RF, et al. Cavernous malformations of the brainstem: experience with 100 patients. *J Neurosurg* 1999;90(01):50–58
- Dashti SR, Hoffer A, Hu YC, Selman WR. Molecular genetics of familial cerebral cavernous malformations. *Neurosurg Focus* 2006;21(01):e2
- Labauge P, Denier C, Bergametti F, Tournier-Lasserre E. Genetics of cavernous angiomas. *Lancet Neurol* 2007;6(03):237–244
- Choquet H, Pawlikowska L, Lawton MT, Kim H. Genetics of cerebral cavernous malformations: current status and future prospects. *J Neurosurg Sci* 2015;59(03):211–220
- Akers A, Al-Shahi Salman R, Awad IA, et al. Synopsis of guidelines for the clinical management of cerebral cavernous malformations: consensus recommendations based on systematic

- literature review by the Angioma Alliance Scientific Advisory Board Clinical Experts Panel. *Neurosurgery* 2017;80(05):665–680
- 16 Pozzati E, Acciarri N, Tognetti F, Marliani F, Giangaspero F. Growth, subsequent bleeding, and de novo appearance of cerebral cavernous angiomas. *Neurosurgery* 1996;38(04):662–669, discussion 669–670
 - 17 Campbell PG, Jabbour P, Yadla S, Awad IA. Emerging clinical imaging techniques for cerebral cavernous malformations: a systematic review. *Neurosurg Focus* 2010;29(03):E6
 - 18 Rivera PP, Willinsky RA, Porter PJ. Intracranial cavernous malformations. *Neuroimaging Clin N Am* 2003;13(01):27–40
 - 19 Zabramski JM, Wascher TM, Spetzler RF, et al. The natural history of familial cavernous malformations: results of an ongoing study. *J Neurosurg* 1994;80(03):422–432
 - 20 de Souza JM, Domingues RC, Cruz LC Jr, Domingues FS, lasbeck T, Gasparetto EL. Susceptibility-weighted imaging for the evaluation of patients with familial cerebral cavernous malformations: a comparison with T2-weighted fast spin-echo and gradient-echo sequences. *AJNR Am J Neuroradiol* 2008;29(01):154–158
 - 21 Haller S, Vernooij MW, Kuijper JPA, Larsson EM, Jäger HR, Barkhof F. Cerebral microbleeds: imaging and clinical significance. *Radiology* 2018;287(01):11–28
 - 22 Menzler K, Chen X, Thiel P, et al. Epileptogenicity of cavernomas depends on (archi-) cortical localization. *Neurosurgery* 2010;67(04):918–924
 - 23 Sone JY, Hobson N, Srinath A, et al. Perfusion and permeability MRI predicts future cavernous angioma hemorrhage and growth. *J Magn Reson Imaging* 2022;55(05):1440–1449
 - 24 Kivelev J, Laakso A, Niemelä M, Hernesniemi J. A proposed grading system of brain and spinal cavernomas. *Neurosurgery* 2011;69(04):807–813, discussion 813–814
 - 25 Ellis JA, Barrow DL. Supratentorial cavernous malformations. *Handb Clin Neurol* 2017;143:283–289
 - 26 Kan P, Tubay M, Osborn A, Blaser S, Couldwell WT. Radiographic features of tumefactive giant cavernous angiomas. *Acta Neurochir (Wien)* 2008;150(01):49–55, discussion 55
 - 27 Lawton MT, Vates GE, Quinones-Hinojosa A, McDonald WC, Marchuk DA, Young WL. Giant infiltrative cavernous malformation: clinical presentation, intervention, and genetic analysis: case report. *Neurosurgery* 2004;55(04):979–980
 - 28 Yu Q, Lin K, Liu Y, Li X. Clinical uses of diffusion tensor imaging fiber tracking merged neuronavigation with lesions adjacent to corticospinal tract: a retrospective cohort study. *J Korean Neurosurg Soc* 2020;63(02):248–260
 - 29 Sarbu N, Pujol T, Oleaga L. Hyperintense perilesional edema in the brain on T1-weighted images: cavernous malformation or metastatic melanoma? Three case reports and literature review. *Neuroradiol J* 2016;29(01):52–56
 - 30 Yun TJ, Na DG, Kwon BJ, et al. A T1 hyperintense perilesional signal aids in the differentiation of a cavernous angioma from other hemorrhagic masses. *AJNR Am J Neuroradiol* 2008;29(03):494–500
 - 31 Kuroedov D, Cunha B, Pamplona J, Castillo M, Ramalho J. Cerebral cavernous malformations: typical and atypical imaging characteristics. *J Neuroimaging* 2023;33(02):202–217
 - 32 Pinker K, Stavrou I, Szomolanyi P, et al. Improved preoperative evaluation of cerebral cavernomas by high-field, high-resolution susceptibility-weighted magnetic resonance imaging at 3 tesla: comparison with standard (1.5 T) magnetic resonance imaging and correlation with histopathological findings: preliminary results. *Invest Radiol* 2007;42(06):346–351
 - 33 Yaghi S, Oommen S, Keyrouz SG. Non-aneurysmal perimesencephalic subarachnoid hemorrhage caused by a cavernous angioma. *Neurocrit Care* 2011;14(01):84–85
 - 34 Negoto T, Terachi S, Baba Y, Yamashita S, Kuramoto T, Morioka M. Symptomatic brainstem cavernoma of elderly patients: timing and strategy of surgical treatment. Two case reports and review of the literature. *World Neurosurg* 2018;111:227–234
 - 35 Anqi X, Zhang S, Jiahe X, Chao Y. Cavernous sinus cavernous hemangioma: imaging features and therapeutic effect of Gamma Knife radiosurgery. *Clin Neurol Neurosurg* 2014;127:59–64
 - 36 Hsiang JN, Ng HK, Tsang RK, Poon WS. Dural cavernous angiomas in a child. *Pediatr Neurosurg* 1996;25(02):105–108
 - 37 Ito M, Kamiyama H, Nakamura T, Nakajima H, Tokugawa J. Dural cavernous hemangioma of the cerebellar falx. *Neurol Med Chir (Tokyo)* 2009;49(09):410–412
 - 38 Joshi V, Muzumdar D, Dange N, Goel A. Supratentorial convexity dural-based cavernous hemangioma mimicking a meningioma in a child. *Pediatr Neurosurg* 2009;45(02):141–145
 - 39 Gonzalez LF, Lekovic GP, Eschbacher J, Coons S, Porter RW, Spetzler RF. Are cavernous sinus hemangiomas and cavernous malformations different entities? *Neurosurg Focus* 2006;21(01):e6
 - 40 Foster KA, Ares WJ, Tempel ZJ, et al. PHACE syndrome is associated with intracranial cavernous malformations. *Childs Nerv Syst* 2016;32(08):1463–1469
 - 41 Yoshinaga T, Yagi K, Morishita T, Abe H, Nonaka M, Inoue T. Cerebral and spinal cavernomas associated with Klippel-Trenaunay syndrome: case report and literature review. *Acta Neurochir (Wien)* 2018;160(02):287–290
 - 42 Brinjikji W, Flemming KD, Lanzino G. De novo formation of a large cavernoma associated with a congenital torcular dural arteriovenous fistula: case report. *J Neurosurg Pediatr* 2017;19(05):567–570
 - 43 Chen DJ, Severson E, Prayson RA. Cavernous angiomas in chronic epilepsy associated with focal cortical dysplasia. *Clin Neuropathol* 2013;32(01):31–36
 - 44 Weigel J, Neher M, Schrey M, Wunsch PH, Steiner HH. Collision tumor composed of meningioma and cavernoma. *J Korean Neurosurg Soc* 2017;60(01):102–107
 - 45 Ma L, Zhang S, Li Z, et al. Morbidity after symptomatic hemorrhage of cerebral cavernous malformation: a nomogram approach to risk assessment. *Stroke* 2020;51(10):2997–3006
 - 46 Dammann P, Wrede K, Jabbarli R, et al. Outcome after conservative management or surgical treatment for new-onset epilepsy in cerebral cavernous malformation. *J Neurosurg* 2017;126(04):1303–1311
 - 47 Davies JM, Kim H, Lawton MT. Surgical treatment of cerebral cavernous malformations. *J Neurosurg Sci* 2015;59(03):255–270
 - 48 Stapleton CJ, Barker FG II. Cranial cavernous malformations: natural history and treatment. *Stroke* 2018;49(04):1029–1035
 - 49 Wen R, Shi Y, Gao Y, et al. The efficacy of Gamma Knife radiosurgery for cavernous malformations: a meta-analysis and review. *World Neurosurg* 2019;123:371–377
 - 50 Peker S, Kiliç T, Sengöz M, Pamir MN. Radiosurgical treatment of cavernous sinus cavernous haemangiomas. *Acta Neurochir (Wien)* 2004;146(04):337–341, discussion 340
 - 51 Kondziolka D, Lunsford LD, Flickinger JC, Kestle JR. Reduction of hemorrhage risk after stereotactic radiosurgery for cavernous malformations. *J Neurosurg* 1995;83(05):825–831